

High-pressure phases of lithia Li_2O : First-principles calculations

K. Kunc,^{1,*} I. Loa,^{1,†} and K. Syassen¹¹Max-Planck-Institut für Festkörperforschung, Heisenbergstrasse 1, D-70569 Stuttgart, Germany

(Received 28 August 2007; revised manuscript received 19 January 2008; published 10 March 2008)

The high-pressure (HP) structural properties of Li_2O are examined theoretically using first-principles calculations (density-functional theory). The calculated results for the HP anticotunnite modification are compared to recent experimental studies. Our main focus is on the hexagonal Ni_2In -type modification, which is a likely candidate for a HP phase of Li_2O at pressures above 100 GPa. The structural aspects of a pressure-induced phase transition from anticotunnite to Ni_2In are characterized in detail; the existence of precursor phenomena is pointed out.

DOI: 10.1103/PhysRevB.77.094110

PACS number(s): 61.50.Ks, 62.50.-p, 77.80.Bh

I. INTRODUCTION

Lithia, Li_2O , is one of the main components of special-purpose glasses and also a material relevant for fusion reactor technology. As a consequence, Li_2O has been dealt with by a variety of theoretical methods, addressing, for instance, diffusion processes and Frenkel defects,¹ properties of clusters,² and elastic properties.³ It is then not surprising that questions concerning its structural behavior at high pressures are being raised. An important problem in this context is the identification of phase transitions and the pressure dependence of physical properties.

In previous work⁴ we have evidenced, experimentally and theoretically, the pressure-induced phase transition in Li_2O , from the cubic antifluorite to orthorhombic anticotunnite structure (space group 62, $Pnma$, $Z=4$ formula units), at pressures between 45 and 50 GPa (experiment) or at 36.9 GPa (first-principles calculations). We have characterized the high-pressure structure, found its basic structural properties and equation of state (EOS) parameters, and determined the evolution of internal structural parameters with applied pressure. More recently, Lazicki *et al.*⁵ brought forth more abundant experimental data which situate the transition at 50 ± 5 GPa. Although not immediately evident from the structure description given by Lazicki *et al.*, their main conclusions agree with the earlier results. Yet, in a few points their data appear to indicate disagreement.

In the present paper, we first briefly examine both works on the anticotunnite modification. The main point addressed here is the possibility of a phase transition to the hexagonal Ni_2In structure (space group 194, $P6_3/mmc$, $Z=2$) at higher pressures. That structure type is a very likely candidate, based on the systematics of crystal structures of ionic AX_2 compounds.⁶ Also, a hexagonal arrangement, although heavily distorted, is inherently present in the orthorhombic anticotunnite modification, cf. Fig. 1. We investigate theoretically the structural stability of anticotunnite Li_2O at pressures above 100 GPa.

II. METHOD OF CALCULATION

The numerical work presented here proceeds along the same lines as in Ref. 4: density functional theory (DFT) in the generalized gradient approximation (GGA),⁷ plane-wave

basis and projector augmented waves (PAW) potentials,⁸ using the VASP codes.⁹ One notable exception: in the present work we chose for the PAW potential of Li one which treats also the $1s^2$ electrons as valence ones. [The latter were counted to the frozen core of Li in Ref. 4, and their eventual effects were accounted for indirectly through the nonlinear core-correction (NLCC).¹⁰] Although the tests performed in Ref. 4 in the context of the antifluorite structure did *not* suggest the explicit treatment of the $1s^2$ shell to be necessary, we now preferred adopting the explicit treatment as a precaution, for the present calculations cover the pressure range of several hundreds of GPa. We use the plane-wave cutoff $E_{\text{pw}}=875$ eV and the k -point sampling of the reciprocal space is now (i.e., for Ni_2In) performed on a $6 \times 6 \times 4$ homogeneous mesh of the Monkhorst-Pack type¹¹ while assuming insulating behavior throughout. We checked, at several representative volumes between 8.75 and 27.5 Å³/ Li_2O and throughout the Brillouin zone (on all the 21 k points of the Monkhorst-Pack mesh), that, indeed, the Ni_2In structure is not metallic; its DFT-GGA energy gap *increases* with pressure. It is useful to note that pressure $P(V)$ is obtained within the DFT formalism at the same time as total energy $E(V)$ but independently: the values of P (as well as other derivatives

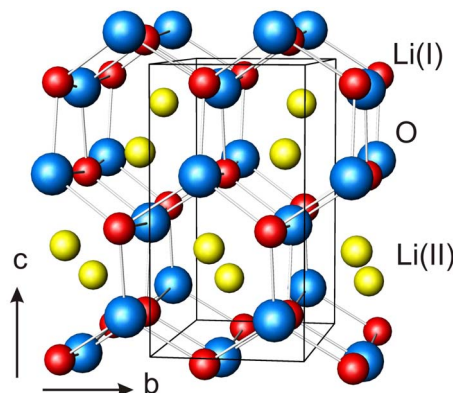


FIG. 1. (Color online) The orthorhombic anticotunnite structure of Li_2O viewed down the a -axis ($Pnma$). Atoms are connected by lines in order to indicate that a hexagonal structural arrangement is preformed in this modification. Lattice constants and atom positions correspond to experimental data of Ref. 4 (see also first set of data listed in Table I).

of energy) are calculated directly, using the stress theorem.¹² The EOS parameters (volume V_0 , bulk modulus B_0 , and pressure derivative B'_0 , all at zero pressure) can be derived from both the $E(V)$ and $P(V)$ data and the results of both approaches will be reported here.

III. ANTICOTUNNITE PHASE

All data on the low-pressure antiferroite structure presented in Ref. 5 are in excellent agreement with our results in Ref. 4. At first sight, one cannot say the same about the results on the anticotunnite modification. One notices a pronounced dissimilarity between the calculated and experimental structural data of Ref. 4 and the experimental data of Ref. 5. Although the lattice constants a , b , and c at 61.9 GPa quoted in Table I of Ref. 5 agree well with the values at $V=16.70 \text{ \AA}^3/\text{Li}_2\text{O}$ in Fig. 3 of Ref. 4, some of the fractional coordinates $x_1 \cdots z_3$ given in the same table differ largely, so that one has to ask whether the same modification has been dealt with in both works or whether a different *description* has been used.

Starting from the structure defined in Table I of Ref. 5, we find that by (a) turning the $(\text{Li}_2\text{O})_4$ “motive” by 180° around the $[a,0,0]$ axis, (b) then shifting it by $[a/2,0,0]$ in the $[1,0,0]$ direction, (c) and changing the numbering in every group of four equivalent atoms, one obtains a description as given in Table I. The transformation is $x=-x'(\text{mod } 1)$; $y=y'$; $z=0.5-z'(\text{mod } 1)$, and the groups Li(1) and Li(2) of Ref. 5 go, respectively, into Li(II) and Li(I) of Ref. 4. The experimental data of Ref. 5 transformed in this way are now in excellent to moderate agreement with the calculated data at $V=16.70 \text{ \AA}^3/\text{Li}_2\text{O}$ (Fig. 3 of Ref. 4). While the difference between $z_3=0.195$ and $z_3=0.1774$ is small, the main discrepancy which still remains is in $x_3=0.117$ which compares imperfectly with $x_3=0.0226$ extracted from Ref. 4.

We considered the possibility of having at hand a distinct structural variant, i.e., one corresponding to a different minimum in $E_{\text{tot}}(x_1 \cdots z_3)$. This possibility was checked by starting energy minimizations from different initial values, viz., those suggested by the modified description (see Table I of the data of Ref. 5). We also tried several other starting points at which the differences in x_3 and z_3 were even more pronounced. In all cases we found considerable forces on atoms ($1-2 \text{ eV/\AA}$), and the optimization algorithms always steered the iterations to the values of $x_1 \cdots z_3$ we obtained previously.⁴ We conclude that the discrepancies in the positional parameters x_3 and z_3 go on the account of a disagreement between measurements and/or analysis of Ref. 5 and calculations as well as measurements and/or analysis of Ref. 4; they do not correspond to any “second variant” of the anticotunnite structure.

As the anticotunnite structures studied appear to be the same in both Refs. 4 and 5, the main unexplained difference is in the bulk modulus B_0 : the anticotunnite modification was found to be much less compressible in the experiment⁵ ($B_0=188 \text{ GPa}$) than in the calculation⁴ ($B_0=80 \text{ GPa}$). This disagreement persists; it perhaps goes on account of the large backextrapolation applied to a relatively small stretch

TABLE I. The orthorhombic anticotunnite structure of Li_2O studied in Refs. 4 and 5, all described in the same $Pnma$ setting as used in Ref. 4. The volume V is for one formula unit ($Z=4$). The Wyckoff sites are $4c$ for O, Li(I), and Li(II). The y coordinate is fixed by symmetry.

Source	$V \text{ (\AA}^3\text{)}$	$a, b, c \text{ (\AA)}$		
Expt. (Ref. 4)	16.70	4.5278		
		2.8003		
		5.2693		
Calc. (Ref. 4)	16.70	4.5296		
		2.7855		
		5.2952		
Expt. (Ref. 5)	16.18	4.456		
		2.7865		
		5.212		
Atom	x	y	z	
O	0.2432	0.25	0.8949	
Li(I)	0.6393	0.25	0.9263	
Li(II)	0.0376	0.25	0.1692	
O	0.2545	0.25	0.8922	
Li(I)	0.6504	0.25	0.9252	
Li(II)	0.0226	0.25	0.1774	
O	0.255	0.25	0.900	
Li(I)	0.695	0.25	0.930	
Li(II)	0.117	0.25	0.195	

of experimental $V(P)$ data obtained under quasihydrostatic conditions.

IV. STABILITY AT MEGABAR PRESSURES: THE Ni_2In PHASE

The coordination number hierarchy of representative ambient- and high-pressure phases of ionic AX_2 compounds⁶ leads us to anticipate the Ni_2In structure to come next when pressure is further increased.⁴ Direct transitions between the cotunnite and the Ni_2In structure types have actually been observed in AX_2 compounds, e.g., in BaF_2 .¹³ Also, an extensive global search performed recently on alkali metal oxides¹⁴ suggests the Ni_2In structure to be a highly probable candidate for Li_2O at pressures in the megabar range (see Fig. 1 in Ref. 14).

Here, we examine the possible transition of Li_2O to the Ni_2In modification in some detail, in particular, from the point of view of the energetics relative to anticotunnite. The hexagonal structure of Ni_2In (space group $P6_3/mmc$, $Z=2$ formula units per elementary unit cell) is described by two lattice parameters a and c and, at any given volume, there is only one parameter to be determined by energy minimization, viz., c/a . All atomic positions are fixed by symmetry.

When optimizing the Ni_2In -type structure at any given volume we start from the results obtained at the nearest

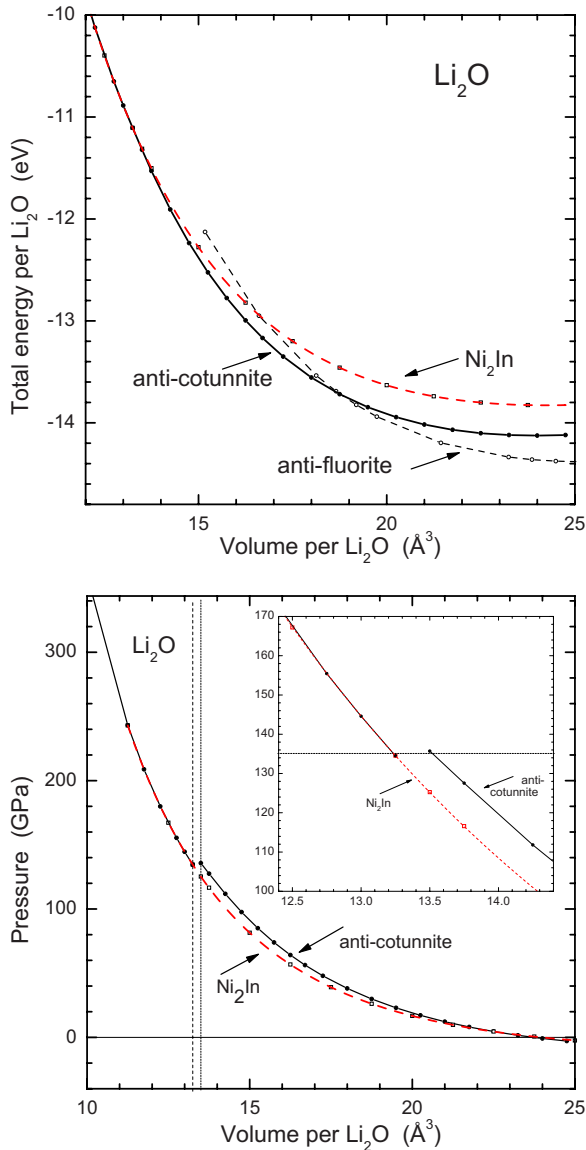


FIG. 2. (Color online) Calculated $E(V)$ and $P(V)$ relations of different phases of Li_2O : anti-fluorite (low-pressure structure, cubic), anti-cotunnite (medium-pressure phase, orthorhombic), and Ni_2In (the hypothetical high-pressure phase, hexagonal).

larger volume. In the very first iteration, we allowed for a sufficiently large variation of the c/a ratio. The calculated $E(V)$ and $P(V)$ data pertinent to the Ni_2In structure are shown in Fig. 2 and the corresponding values of the axial ratio are given in Fig. 3 (labeled $c_{\text{hex}}/a_{\text{hex}}$). An excellent fit of all the calculated $E(V)$ and $P(V)$ points in the interval $(11.25; 25.0) \text{ \AA}^3/\text{Li}_2\text{O}$ was obtained by the Holzapfel equation of state¹⁵ and the basic elastic properties thus obtained are given in Table II together with the data from our earlier study. We notice that the Ni_2In modification at its equilibrium V_0 is *softer* than the anti-cotunnite one at the same volume (B_0 smaller by $\approx 25\%$), but it *hardens* with pressure *faster* ($B' \approx 4.6$ as compared to ≈ 4.0).

When comparing in Fig. 2 with the $E(V)$ variation of the anti-cotunnite modification,⁴ we see immediately that instead of intersecting, the anti-cotunnite and Ni_2In curves *merge* at

small volumes. Whereas at low and moderate pressures the anti-cotunnite structure is preferred to the Ni_2In one by hundreds of meV/ Li_2O , at volumes smaller than $\sim 13 \text{ \AA}^3/\text{Li}_2\text{O}$ the energetics does *not* favor one structure against the other. Consistent information is obtained by evaluating the enthalpies $H = E + PV$: $\Delta H = 0$ at all pressures above $P_t = 135 \text{ GPa}$.

The configuration of the two $E(V)$ variations in Fig. 2, although somewhat unusual, is by no means insensible. In principle, a continuous transition between the anti-cotunnite and Ni_2In structures is possible because of a group-subgroup relation between Ni_2In (space group $P6_3/mmc$) and anti-cotunnite ($Pnma$). In other words, the hexagonal structure can be described within the orthorhombic system. This involves a doubling of the unit cell. The relevant relations are (within our choice of axes and basis) $a = c_{\text{hex}}$, $b = a_{\text{hex}}$, and $c = \sqrt{3}a_{\text{hex}}$, and the fractional coordinates $x_1 \cdots z_3$ take the values $11/12$, $3/4$, $1/4$, and 0 , respectively, and these are invariable and defined by symmetry (see also Ref. 13).

Zooming in at the “confluence” of the two $E(V)$ curves in Fig. 2 confirms the coincidence of the two variations at small volumes—and it suggests that it would be rather difficult to determine the actual transition point with any accuracy from the $E(V)$ calculations alone: these variations are found to be almost continuous (within the resolution of the calculations). The corresponding $P(V)$ equation of state, which is also shown in Fig. 2, is more explicit on this matter and it situates the transition quite clearly at $\approx 135 \text{ GPa}$ where the volume changes discontinuously by about -1.9% , from 13.5 to $13.25 \text{ \AA}^3/\text{Li}_2\text{O}$. The discontinuity ascertains that we are dealing with a first-order transition.

In Fig. 3 we plot ratios of the optimized anti-cotunnite lattice constants a/b and c/b and their variation with decreasing volume. One observes a pronounced nonlinearity at volumes approaching $13.5 \text{ \AA}^3/\text{Li}_2\text{O}$, followed by an *abrupt change* (on the quite narrow volume grid of the calculations) in both a/b and c/b . At $V = 13.25 \text{ \AA}^3/\text{Li}_2\text{O}$ the transition to the new phase is completed and further compression causes the c/b and a/b to evolve with *different slopes*. In particular, we observe that the evolution of the a/b of anti-cotunnite at small volumes is a smooth continuation of the ratio $c_{\text{hex}}/a_{\text{hex}}$ of the Ni_2In structure, and that also the c/b assumes the value characteristic of the Ni_2In structure: $\sqrt{3}$ (a constant). The transition thus can be situated also from the evolution of structural parameters, between 13.5 and $13.25 \text{ \AA}^3/\text{Li}_2\text{O}$, and the abruptness of the changes in Fig. 3 support the notion that we encounter a *first-order* transition. The abrupt changes in c/b and a/b amount to -6.7% and -12.2% , respectively. Various parameters pertinent to the phase transition are collected in Table III.

Upon *increasing* the volume, one expects the transition to the Ni_2In modification to be reversible and to bring the system back to its original atomic structure. However, in pursuing the iterations also “from left to right” in Fig. 3, we noticed that the system can remain trapped in the Ni_2In -type structure if only small variations of structural parameters are allowed for. Part of this evolution is indicated by the three isolated solid circles at around $14 \text{ \AA}^3/\text{Li}_2\text{O}$ belonging to the c/b and a/b variations. The chances that these values of lattice parameters describe a really existing structure (i.e.,

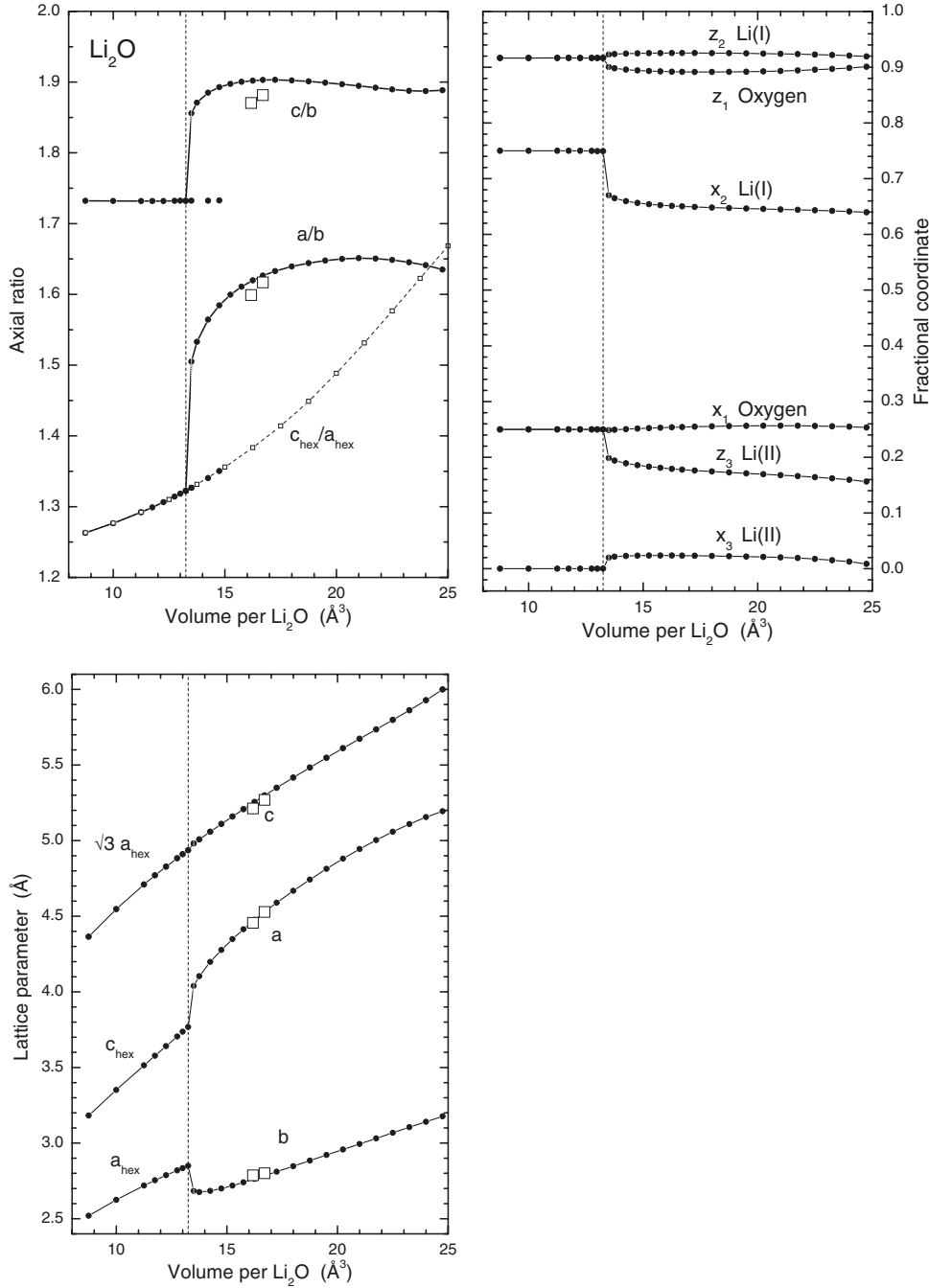


FIG. 3. The evolution under pressure of the lattice constants (a , b , and c -orthorhombic; a_{hex} and c_{hex} -hexagonal) and the internal structural parameters ($x_1 \cdots z_3$ of anticotunnite) of Li_2O . Pronounced discontinuities are observed between 13.25 and 13.5 $\text{\AA}^3/\text{Li}_2\text{O}$. The solid lines connecting the axial ratio data correspond to the true minima of the total energy while the few isolated solid symbols around 14 $\text{\AA}^3/\text{Li}_2\text{O}$ were obtained by structural optimization at increasing volumes within a narrow parameter space. Open symbols represent the subset of experimental data from Table I (Refs. 4 and 5).

two coexisting phases) are nevertheless slim because the ΔE^{tot} increases very rapidly from one point to another: initially zero at $V=13.25 \text{ \AA}^3/\text{Li}_2\text{O}$, the energy difference Ni_2In (metastable or unstable)—anticotunnite (stable) reaches 93 meV/ Li_2O at $14.75 \text{ \AA}^3/\text{Li}_2\text{O}$, and it keeps increasing rapidly with further increase of volume.

The actual values of the calculated lattice constants a , b , and c and optimized fractional coordinates $x_1 \cdots z_3$ of the anticotunnite modification at pressures prior to and following the transition are displayed in Fig. 3 as well. The nonsmoothness of their variation and eventually changes in slope are seen at the same volumes as those of c/b and a/b . All fractional coordinates converge to the values corresponding to the Ni_2In structure; the “degeneracies” that we notice in some of them (x_1 and z_3 becoming equal, similarly

$z_1=z_2, \dots$), are consequence of the additional symmetries imposed by the Ni_2In structure.

V. CONCLUSIONS

Our conclusions are as follows: (1) The structure of anticotunnite-type high-pressure Li_2O reported by Lazicki *et al.*⁵ is basically identical to that of Kunc *et al.*,⁴ except for a small discrepancy in one of the internal structural parameters (x_3). (2) The upper pressure limit for the stability of anticotunnite Li_2O is predicted to be 135 GPa ($T=0$ K). At that pressure value, anticotunnite Li_2O would transform to the densely packed Ni_2In structure, provided that there is no competition of some lower-symmetry structure with an effec-

TABLE II. Summary of the calculated equation of state parameters for three modifications of Li₂O taken from Ref. 4 and the present work. Throughout, the Holzapfel EOS (Ref. 15) was used to fit the calculated data (e.g., 12 volumes in the interval 11.25–25.0 Å³/Li₂O in the case of the Ni₂In structure). The quoted errors correspond to the purely statistical uncertainties for 90% confidence.

Phase	Source	Data	V_0 (Å ³)	B_0 (GPa)	B'
Antifluorite	Ref. 4	$E(V)$	24.95(1)	79.9(4)	4.02(2)
		$P(V)$	24.74(2)	81.1(8)	4.06(4)
Anticotunnite	Ref. 4 and this work	$E(V)$	23.71(3)	77.6(9)	4.08(5)
		$P(V)$	23.52(5)	79.7(17)	4.04(7)
Ni ₂ In	This work	$E(V)$	24.26(3)	59.0(6)	4.57(2)
		$P(V)$	23.98(3)	61.3(5)	4.55(2)

tive coordination number intermediate between 9 (anticotunnite) and 11 (Ni₂In). (3) Although a group-subgroup relationship exists for the anticotunnite and Ni₂In structures and, further, the predicted volume change at the phase transition is rather small, the transition is considered to be of first order (at $T=0$ K), as is also indicated by abrupt variations of lattice constants and internal structural parameters. (4) Upon approaching the phase transition, the variation of lattice constants and positional parameters of the anticotunnite variant exhibits pronounced nonlinearities. This behavior can be considered as a precursor of the phase transition, and the nonlinearities should also be reflected in the variations of phonon frequencies with pressure. In this respect, anomalies may be detectable by vibrational spectroscopy, viz., as a softening of phonon mode frequencies of anticotunnite. (5) The results for Li₂O reported here suggest that studies of high-pressure structural transitions from anticotunnite to Ni₂In in AX₂ compounds deserve a careful investigation of the structural and lattice-dynamical properties in the vicinity of the phase transition. Obvious candidates would be BaF₂ (Ref. 13) and CaF₂.¹⁶ (6) Locating the anticotunnite to Ni₂In tran-

TABLE III. Quantities pertinent to the calculated anticotunnite → Ni₂In phase transition of Li₂O at 135 GPa. The Ni₂In modification (lower block) is described in the orthorhombic setting and all parameters are optimized in that setting. If transformed to the hexagonal setting, the lattice parameters are $a_{\text{hex}}=2.8540$ Å and $c_{\text{hex}}=3.7776$ Å and all atom coordinates are fixed by symmetry. The relative volume change at the phase transition amounts to −1.9%.

	V (Å ³)	a, b, c (Å)	
a-cot.	13.50	4.0392	
		2.6840	
		4.9810	
Ni ₂ In	13.25	3.7678	
orthorh.		2.8496	
		4.9363	
Atom	x	y	z
O	0.2486	0.25	0.9004
Li(I)	0.6703	0.25	0.9228
Li(II)	0.0198	0.25	0.1985
O	0.2500	0.25	0.9167
Li(I)	0.7494	0.25	0.9167
Li(II)	0.0001	0.25	0.2496

sition of Li₂O at ~135 GPa probably means that a further transition to a post-Ni₂In-type modification as observed in dihydrides¹⁷ lies outside the current range of static high-pressure techniques.

ACKNOWLEDGMENT

Part of the computer resources used in this work were provided by the Scientific Committee of Institut du Développement et des Ressources en Informatique Scientifique (IDRIS), Orsay, France.

*Permanent address: Institut des NanoSciences de Paris, CNRS, Université Pierre et Marie Curie-Paris 6, and Université Denis Diderot-Paris 7, 140 rue de Lourmel, F-75015 Paris, France; kunc@ccr.jussieu.fr

†Present address: The University of Edinburgh, School of Physics and Centre for Science at Extreme Conditions, Mayfield Road, Edinburgh EH9 3JZ, United Kingdom.

¹R. Shah, A. DeVita, V. Heine, and M. C. Payne, Phys. Rev. B **53**, 8257 (1996) and references therein.

²F. Finocchi and C. Noguera, Eur. Phys. J. D **9**, 327 (1999) and references therein.

³R. Dovesi, C. Roetti, C. Freyria-Fava, M. Prencipe, and V. R. Saunders, Chem. Phys. **156**, 11 (1991).

⁴K. Kunc, I. Loa, A. Grzechnik, and K. Syassen, Phys. Status Solidi B **242**, 1857 (2005).

⁵A. Lazicki, C.-S. Yoo, W. J. Evans, and W. E. Pickett, Phys. Rev. B **73**, 184120 (2006).

⁶J. M. Leger and J. Haines, Eur. J. Solid State Inorg. Chem. **34**, 785 (1997).

⁷J. P. Perdew and Y. Wang, Phys. Rev. B **45**, 13244 (1992).

⁸P. E. Blöchl, Phys. Rev. B **50**, 17953 (1994); G. Kresse and D. Joubert, *ibid.* **59**, 1758 (1999).

⁹G. Kresse and J. Hafner, Phys. Rev. B **47**, R558 (1993); G. Kresse, Ph.D. thesis, Technische Universität Wien, 1993; G. Kresse and J. Furthmüller, Comput. Mater. Sci. **6**, 15 (1996); Phys. Rev. B **54**, 11169 (1996).

¹⁰S. G. Louie, S. Froyen, and M. L. Cohen, Phys. Rev. B **26**, 1738 (1982).

¹¹H. J. Monkhorst and J. D. Pack, Phys. Rev. B **13**, 5188 (1976).

¹²O. H. Nielsen and R. M. Martin, Phys. Rev. Lett. **50**, 697 (1983);

- Phys. Rev. B **32**, 3780 (1985).
- ¹³J. M. Leger, J. Haines, A. Atouf, O. Schulte, and S. Hull, Phys. Rev. B **52**, 13247 (1995).
- ¹⁴Z. Cancarevic, J. C. Schön, and M. Jansen, Phys. Rev. B **73**, 224114 (2006).
- ¹⁵W. B. Holzapfel, Rep. Prog. Phys. **59**, 29 (1996). The pressure-volume relation (labeled HO2) is given by $P(V)$
- $= 3B_0 X^{-n}(1-X)\exp[\eta(1-X)]$ where $X=(V/V_0)^{1/3}$, $\eta=3B'_0/2 + 1/2 - n$, and $n=5$. The corresponding analytical form of the energy-volume relation is obtained by integration.
- ¹⁶Xiang Wu, Shan Qin, and Ziyu Wu, Phys. Rev. B **73**, 134103 (2006).
- ¹⁷K. Kinoshita, M. Nishimura, Y. Akahama, and H. Kawamura, Solid State Commun. **141**, 69 (2007).